Chirikov standard map

Boris Chirikov and Dima Shepelyansky (2008), Scholarpedia, 3(3):3550. doi:10.4249/scholarpedia.3550 revision #192427 [link to/cite this article]

- **Dr. Boris Chirikov**, Budker Institute of Nuclear Physics, Novosibirsk, Russia
- **Dima Shepelyansky**, Laboratoire de Physique Théorique, CNRS, Université Paul Sabatier, Toulouse

The **Chirikov standard map** [1], [2] is an area-preserving map for two canonical dynamical variables, i.e., momentum and coordinate (p, x). It is described by the equations:

$$\begin{aligned} \bar{p} &= p + K \sin x \\ \bar{x} &= x + \bar{p} \end{aligned} \qquad (1)$$

where the bars indicate the new values of variables after one map iteration and K is a dimensionless parameter that influences the degree of chaos. Due to the periodicity of $\sin x$ the dynamics can be considered on a cylinder (by taking $x \mod 2\pi$) or on a torus (by taking both $x, p \mod 2\pi$). The map is generated by the time dependent Hamiltonian $H(p, x, t) = p^2/2 + K \cos(x)\, \delta_1(t)$, where $\delta_1(t)$ is a periodic $\delta-$function with period 1 in time. The dynamics is given by a sequence of free propagations interleaved with periodic kicks.

Examples of the Poincare sections of the standard map on a torus are shown in the following Figs. 1,2,3.

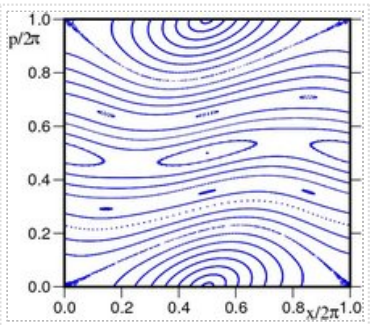

Figure 1: K=0.5

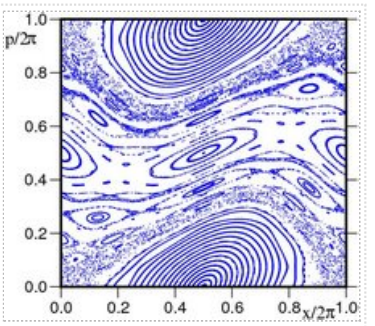

Figure 2: K=0.971635

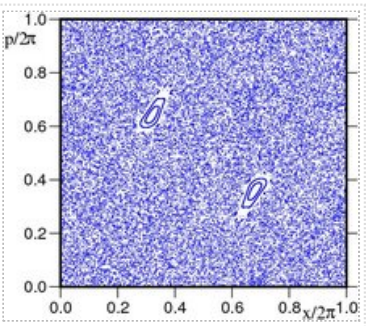

Figure 3: K=5

Below the critical parameter $K < K_c$ (Fig.1) the invariant Kolmogorov-Arnold-Moser (KAM) curves restrict the variation of momentum p to be bounded. The golden KAM curve with the rotation number

$$r = r_g = (\sqrt{5} - 1)/2 = 0.618033...$$

is destroyed at $K = K_g = 0.971635...$ [3], [4] (Fig.2). This Fig. shows a generic phase space structure typical for various area-preserving maps with smooth generating functions: stability islands are embedded in a chaotic sea, similar structure appears on smaller and smaller scales. In a vicinity of a critical invariant curve, with a golden tail in a continued fraction expansion of r, the phase space structure is universal for all smooth maps [4]. Above the critical value $K > K_c$ (see Fig.3 showing a chaotic component and visible islands of stability) the variation of p becomes unbounded and is characterized by a diffusive growth $p^2 \sim D_0 t$ with number of map iterations t. Here D_0 is a diffusion rate with $D_0 \approx (K - K_c)^3/3$ for $K_c < K < 4$ and $D_0 \approx D_{ql} = K^2/2$ for $4 < K$ [2], [5]. There are strong arguments in favor of the equality $K_c = K_g$ but rigorously it is only proven that there are no KAM curves for $K > 63/64 = 0.984375$ [6]. With the numerical results [3], [4] this implies inequality for the global chaos border, $K_g \leq K_c < 63/64$.

A simple analytical criterion proposed in 1959 and now known as the Chirikov resonance-overlap criterion [7] gives the chaos border $K_c = \pi^2/4$ [1] and after some improvements leads to $K_c \approx 1.2$ [2],[8]. This accuracy is not so impressive compared to modern numerical methods but still up to now this criterion remains the only simple analytical tool for determining the chaos border in various Hamiltonian dynamical systems.

The Kolmogorov-Sinai entropy of the map is well described by relation $h \approx \ln(K/2)$ valid for $K > 4$[1], [2].

Contents

Universality and Applications

The map (1) describes a situation when nonlinear resonances are equidistant in phase space that corresponds to a local description of dynamical chaos. Due to this property various dynamical systems and maps can be locally reduced to the standard map and due to this reason the term *standard map* was coined in [2]. Thus, the standard map describes a universal, generic behavior of area-preserving maps with divided phase space when integrable islands of stability are surrounded by a chaotic component. A short list of systems reducible to the standard map is given below:

- chaotic layer around separatrix of a nonlinear resonance induced by a monochromatic force (the whisker map) [2]
- charged particle confinement in mirror magnetic traps [1], [2], [7], [9]
- fast crossing of nonlinear resonance [1], [10]
- particle dynamics in accelerators [11]
- comet dynamics in solar system [12] with a rather similar map for the comet Halley [13]
- microwave ionization of Rydberg atoms (linked to the Kepler map) [14] and autoionization of molecular Rydberg states [15]
- electron magnetotransport in a resonant tunneling diode [16]

Open Problems

- In spite of fundamental advances in ergodic theory [17], a rigorous proof of the existence of a set of positive measure of orbits with positive entropy is still missing, even for specific values of K (see e.g. [18]).
- What are the fractal properties of critical chaos parameter $K_c(r)$ as a function of arithmetic properties of the rotation number r of KAM curve? do local maxima correspond only to a golden tail of continuous fraction expansion [3], [4] or they may have tails with Markov numbers as it is conjectured in [19]? (see also [20])
- Due to trajectory sticking around stability islands the statistics of Poincare recurrences in Hamiltonian systems with divided phase space (see e.g. Fig.2 with a critical golden KAM curve) is characterized by an algebraic decay $P(\tau) \propto 1/\tau^{\alpha}$ with $\alpha \approx 1.5$ while a theory based on the universality in a vicinity of critical golden curve gives $\alpha \approx 3$; this difference persists up to 10^{13} map iterations; as a result correlation functions decay rather slowly $C(\tau) \sim \tau P(\tau) \propto 1/\tau^{\alpha-1}$ that can lead to a divergence of diffusion rate $D \sim \tau C(\tau)$ (see [21] and Refs. therein)

Quantum Map

The quantization of the standard map is obtained by considering variables in (1) as the Heisenberg operators with the commutation relation $[p, x] = -i\hbar$, where $\hbar$ is an effective dimensionless Planck constant. In a same way it is possible to use the Schrödinger equation with the Hamiltonian $H(\hat{p}, \hat{x}, t)$ given above and $\hat{p} = -i\hbar\partial/\partial x$. Integration on one period gives the quantum map for the wave function ψ:

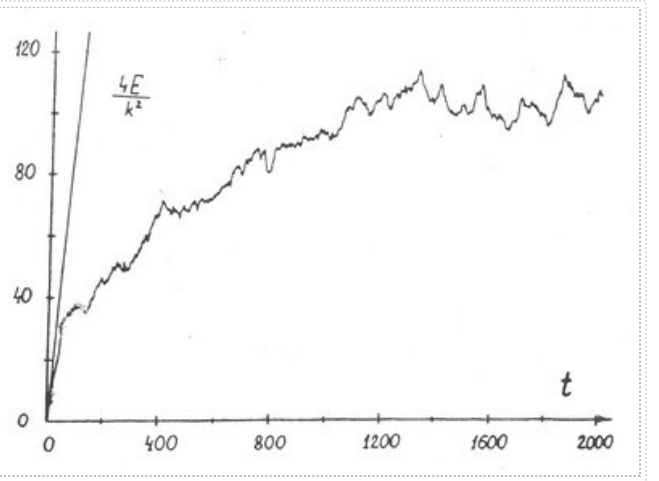

Figure 4: Dependence of rescaled rotator energy $E/(k^2/4)$ on time t for $K = kT = 5, \hbar = 0.25 (k = 20, T = 0.25)$; the full curve shows numerical data and the straight line gives the diffusive energy growth in the classical case (from [23]).

$$\bar{\psi} = \hat{U}\psi = e^{-i\hat{p}^2/2\hbar} e^{-iK/\hbar \cos \hat{x}} \psi \tag{2}$$

where bar marks the new value of ψ after one map iteration. Due to space periodicity of the Hamiltonian the momentum can be presented in the form $p = \hbar(n + \beta)$, where n is an integer and β is a quasimomentum preserved by the evolution operator $\hat{U}$. The case with $\beta = 0$ corresponds to a periodic boundary conditions with $\psi(x + 2\pi) = \psi(x)$ and is known as the kicked rotator introduced in [22].

Other notations with $\hbar \to T$, $K/\hbar \to k$ are also used to mark the dependence on the period T between kicks, then $K = kT$. The diffusion rate over quantum levels n is $D = D_0/\hbar^2 = n^2/t \approx K^2/2\hbar^2 = k^2/2$, thus the rotator energy $E =< n^2 > /2$ grows linearly with time. Quantum interference effects lead to a suppression of this semiclassical diffusion [22] on the diffusive time scale t_D so that the quantum probability spreads effectively only on a finite number of states $\Delta n \sim \sqrt{Dt_D}$ (Fig.4). According to the analytical estimates obtained in [23]:

$$t_D \sim \Delta n \sim D \sim k^2 \sim D_0/\hbar^2. \tag{3}$$

This diffusive time scale is much larger than the Ehrenfest time scale [23], [24] $t_E \sim \ln(1/\hbar)/2h$ after which a minimal coherent wave packet spreads over the whole phase space due to the exponential instability of classical dynamics. For $t < t_E$ a quantum wave packet follows the chaotic dynamics of a classical trajectory as it is guaranteed by the Ehrenfest theorem [23]. For the case of Fig.4 the Kolmogorov-Sinai entropy $h \approx 1$ and the Ehrenfest time $t_E \sim 1$ is extremely short comparing to the diffusive time $t_D \sim D \sim 200$. The quantum suppression of chaotic diffusion is similar to the Anderson localization in disordered systems if to consider the level number as an effective site number in a disordered lattice, such an analogy has been established in [25]. However, in contrast to a disordered potential for the case of Anderson localization, in the quantum map (2) diffusion and chaos have a pure deterministic origin appearing as a result of dynamical chaos in the classical limit.

Due to that this phenomenon is called the dynamical localization. The eigenstates of the unitary evolution operator $\hat{U}$ are exponentially localized over momentum states $\psi_m(n) \sim \exp(-|n - m|/l)/\sqrt{l}$ with the localization length $l \sim \Delta n \sim t_D$ given by the relation [26], [27]

$$l = D(K)/2 = D_0(K)/2\hbar^2, \tag{4}$$

where D is the semiclassical diffusion expressed via a square number of levels per period of perturbation. For $\hbar = T > 1$ the chaos parameter K in the dependence $D(K)$ should be replaced by its quantum value $K \to K_q = 2k \sin T/2$ [27]. The quantum localization length l repeats the

characteristic oscillations of the classical diffusion as it is shown in Fig.5. The relation (4) assumes that $T/4\pi$ is a typical irrational number while for rational values of this ratio the phenomenon of quantum resonance takes place and the energy grows quadratically with time for rational values of quasimomentum [28]. The derivations of the relation (4) based on the field theory methods applied to dynamical systems with chaotic diffusion can be find in [29], [30] (see also Refs. therein).

If the quantum map (2) is taken on a torus with N levels then the level spacing statistics is described by the Poisson law for $N \gg l$ and by the Wigner-Dyson law of the random matrix theory for $N \ll l$ [24],[31]. In the later case the quantum eigenstates are ergodic on a torus in agreement with the Shnirelman theorem and the level spacing statistics agrees with the Bohigas-Giannoni-Schmit conjecture (see books on quantum chaos in Recommended Reading).

The quantum map (2) was built up experimentally with cold atoms in a kicked optical lattice by the Raizen group [32]. Such a case corresponds to a particle in an infinite periodic lattice with averaging over many various β. The quantum resonances at $\beta \approx 0$ were also experimentally observed with the Bose-Einstein condensate (BEC) in [33]. Quantum accelerator modes for kicked atoms falling in the gravitational field were found and analyzed in [34].

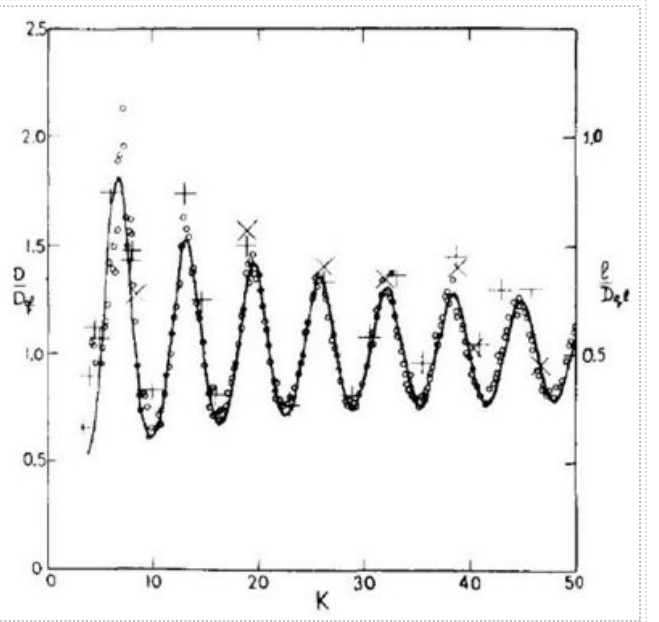

Figure 5: Dependence of the localization length l on the quantum parameter of chaos $K \to K_q = 2k \sin T/2$. The circles and the curve are, respectively, the numerical data and the theory for the classical diffusion $D(K)$ (see [8]). The quantum data for l are shown by + (for $0 < T < \pi$) and by × (for $\pi < T < 2\pi$); here $k = 30$; $D_{ql} = k^2/2$ (from [27]).

Extensions and Related Quantum Systems

Due to universal properties of the standard map its quantum version also finds applications for various systems and various physical effects:

- dynamical localization for ionization of excited hydrogen atoms in a microwave field

was theoretically predicted in [35] and was experimentally observed by the group of P.Koch [36] (see more details in [14],[37],[38])

- quantum particle in a triangular well and monochromatic field with a quantum delocalization transition [39]
- the kicked Harper model where in contrast to the relation (4) the quantum delocalization can take place due to quasi-periodicity of unperturbed spectrum (see [40], [41] and Refs. therein)
- 3D Anderson transition in kicked rotator with modulated kick strength and quantum transport in mesoscopic conductors (see [42] and Refs. therein)
- dissipative quantum chaos [43]
- fractal Weyl law for the quantum standard map with absorption (see [44] and Refs. therein)

Time Reversibility and Boltzmann - Loschmidt Dispute

The statistical theory of gases developed by Boltzmann leads to macroscopic irreversibility and entropy growth even if dynamical equations of motion are time reversible. This contradiction was pointed out by Loschmidt and is now known as the Loschmidt paradox. The reply of Boltzmann relied on the technical difficulty of velocity reversal for material particles: a story tells that he simply said "then go and do it" [45]. The modern resolution of this famous dispute, which took place around 1876 in Wien, came with the development of the theory of dynamical chaos (see e.g. [8], [17]). Indeed, for chaotic dynamics the Kolmogorov-Sinai entropy is positive and small perturbations grow exponentially with time, making the motion practically irreversible. This fact is convenient to illustrate on the example of the standard map which dynamics is time reversible, e.g. by inverting all velocities at the middle of free propagation between two kicks (see Fig.6). This explanation is valid for

classical dynamics, while the case of quantum dynamics requires special consideration. Indeed, in the quantum case the exponential growth takes place only during the rather short Ehrenfest time, and the quantum evolution remains stable and reversible in presence of small perturbations [46] (see Fig.7). Quantum reversibility in presence of various perturbations has been actively studied in recent years and is now described through the Loschmidt echo (see [47] and Refs. therein). A method of approximate time reversal of matter waves for ultracold atoms in the regime of quantum chaos, like those in [32], [33], is proposed in [48]. In this method a large fraction of the atoms returns back even if the time reversal is not perfect. This fraction of the atoms exhibits Loschmidt cooling which can decrease their temperature by several orders of magnitude. At the same time a kicked BEC of attractive atoms (soliton) described by the Gross-Pitaevskii equation demonstrates a truly chaotic dynamics for which the exponential instability breaks the time reversibility [49]. However, since a number of atoms in BEC is finite and since BEC is a really quantum object one should expect that the Ehrenfest time is still very short and hence the time reversibility should be preserved in presence of small errors if the second quantization is taken into account.

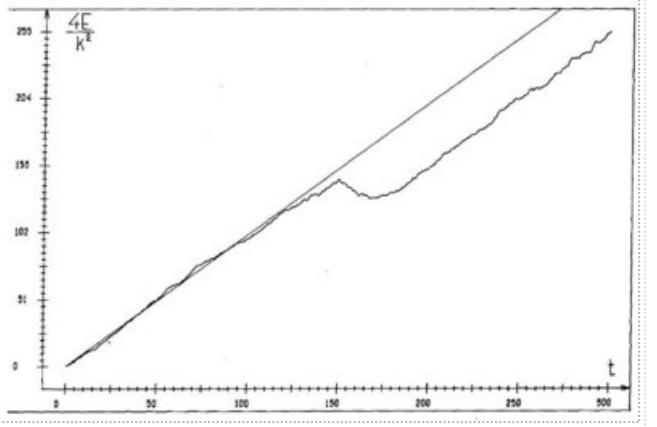

Figure 6: Dependence of rescaled energy $E/(k^2/4)$ on time in the classical map (1) at $K = 5$; time reversal is performed at $t = 150$; numerical simulations are done on BESM-6 with relative accuracy $\epsilon \approx 10^{-12}$ (from [46]).

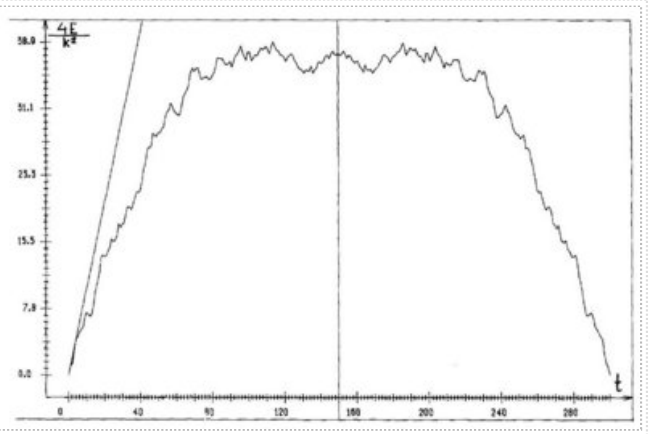

Figure 7: Same as in Fig.6 but for the quantum map (2) with $K = 5, \hbar = 0.25$, the straight line shows the classical diffusion; time reversal is performed at the moment $t = 150$ marked by the vertical line, numerical simulations are done on the same computer BESM-6, in addition random quantum phases $0 < \Delta\phi < 0.1$ are added for quantum amplitudes in momentum representation at the moment of time reversal (from [46]).

Links to Other Physical Topics

Frenkel-Kontorova Model

The Frenkel-Kontorova model describes a one-dimensional chain of atoms/particles with harmonic couplings placed in a periodic potential [50]. This model was introduced with the aim to study crystal dislocations but it also successfully applies for the description of commensurate-incommensurate phase transitions, epitaxial monolayers on the crystal surface, ionic conductors, glassy materials, charge-density waves and dry friction [51]. The Hamiltonian of the model is $H = \sum_i \left(\frac{P_i^2}{2} + \frac{(x_i - x_{i-1})^2}{2} - K \cos x_i \right)$, where P_i, x_i are momentum and position of atom i. At the equilibrium the momenta $P_i = 0$ and $\partial H/\partial x_i = 0$ so that the positions of atoms are described by the map (1) with $p_{i+1} = x_{i+1} - x_i,\ p_{i+1} = p_i + K \sin x_i$. The density of atoms corresponds to the rotation number r of an invariant KAM curve. For the golden density with $r = r_g$ the chain slides in the periodic potential for $K < K_g$ (KAM curve regime) while for $K > K_g$ the transition by the breaking of analyticity, or Aubry transition, takes place, the chain becomes pinned and atoms form an invariant Cantor set called cantorus (see [52] and Aubry-Mather theory). In this regime the phonon spectrum has a gap so that the phonon excitations are suppressed at low temperature. The mathematical Aubry-Mather theory guarantees that the ground state of the chain exists and is unique. However there exist exponentially many static equilibrium configurations which are exponentially close to the energy of the ground state. The energies of these configurations form a fractal quasi-degenerate band structure and become mixed at any physically realistic temperature. Thus, such configurations can be viewed as a dynamical spin glass. For a case of Coulomb interactions between particles (e.g. ions or electrons) one obtains a problem of Wigner crystal in a periodic potential which again is locally described by the Frenkel-Kontorova model since the map (1) gives the local description of the dynamics. For the quantum Frenkel-Kontorova model the dynamics of atoms (ions) in the chain is quantum. In this case the quantum vacuum fluctuations and instanton tunneling lead to a quantum melting of pinned phase: above a certain effective Planck constant a quantum phase transition takes place from pinned instanton glass to sliding phonon gas (see [53] and Refs. therein).

Quantum Computing

One iteration of maps (1) and (2) can be simulated on a quantum computer in a polynomial number of quantum gates for an exponentially large vector representing a Liouville density distribution or a quantum state. The quantum algorithm of such a quantum computation is described in [54], effects of quantum errors are analyzed in [55] (see also Refs. therein).

Historical Notes

The standard map (1) in a form of recursive relation for atoms in a periodic potential appears already in the works of Kontorova and Frenkel [50]. As a dynamical map it first appeared as a description of electron dynamics in a new relativistic accelerator proposed by V.I.Veksler (Dokl. Akad. Nauk SSSR 43: 346 (1944)). The regime of a stable regular acceleration was studied later also by A.A.Kolomensky (Zh. Tekh. Fiz. 30: 1347 (1960)) and S.P.Kapitsa, V.N.Melekhin ("Microtron", Nauka, Moscow (1969) in Russian). Among the early researchers of model (1) was also British physicist J.B.Taylor (unpublished reports). The description of chaos in map (1) and its main properties, including chaos border, diffusion rate and positive entropy, was given in [1]. The term "standard map" appeared in [2], "Chirikov-Taylor map" [8] and "Chirikov standard map" [16] are also used, the quantum standard map or kicked rotator was first considered in [22]. Appearance of other terms: Kolmogorov-Arnold-Moser theory [1], Arnold diffusion [1], Kolmogorov-Sinai entropy [2], Ehrenfest time [24].

Recommended Reading

B.V.Chirikov, "Research concerning the theory of nonlinear resonance and stochasticity", Preprint N 267, Institute of Nuclear Physics, Novosibirsk (1969), (Engl. Trans., CERN Trans. 71-40 (1971))

B.V.Chirikov, "A universal instability of many-dimensional oscillator systems", Phys. Rep. 52: 263 (1979).

B.V.Chirikov, "Time-dependent quantum systems" in "Chaos and quantum mechanics", Les Houches Lecture Series, Vol. 52, pp.443-545, Eds. M.-J.Giannoni, A.Voros, J.Zinn-Justin, Elsevier Sci. Publ., Amsterdam (1991)

A.J.Lichtenberg, M.A.Lieberman, "Regular and chaotic dynamics", Springer, Berlin (1992).

F.Haake, "Quantum signatures of chaos", Springer, Berlin (2001).

L.E.Reichl, "The Transition to chaos in conservative classical systems and quantum manifestations", Springer, Berlin (2004).

Internal references

- James Meiss (2007) Hamiltonian systems. Scholarpedia, 2(8):1943.
- Martin Gutzwiller (2007) Quantum chaos. Scholarpedia, 2(12):3146.

External Links

Selected publications of Boris Chirikov [1] (http://www.quantware.ups-tlse.fr/chirikov/)

Sputnik of Chaos [2] (http://www.quantware.ups-tlse.fr/dima/chirikov.html)

Google query for "standard map" [3] (http://www.google.com/#sclient=psy&q=%22standard+map%22)

References

[1] B.V.Chirikov, "Research concerning the theory of nonlinear resonance and stochasticity", Preprint N 267, Institute of Nuclear Physics, Novosibirsk (1969) [4] (http://www.quantware.ups-tlse.fr/chirikov/refs/chi1969.pdf) , (Engl. Trans., CERN Trans. 71-40 (1971)) [5] (http://www.quantware.ups-tlse.fr/chirikov/refs/chi1969e.pdf) .

[2] B.V.Chirikov, "A universal instability of many-dimensional oscillator systems", Phys. Rep. 52: 263 (1979) [6] (http://www.sciencedirect.com/science?_ob=ArticleURL&_udi=B6TVP-46SPHBD-5V&_user=10&_rdoc=1&_fmt=&_orig=search&_sort=d&view=c&_acct=C000050221&_version=1&_urlVersion=0&_userid=10&md5=14572407bf0c9f49e4b9da787729613a) .

See also

Hamiltonian systems, Mapping, Chaos, Kolmogorov-Arnold-Moser Theory, Kolmogorov-Sinai entropy, Aubry-Mather theory, Quantum chaos

Updates added after 2008

Here some additional features of the standard map, which appeared after 2008 or were omitted in the 2008 article edition, are presented.

Mathematical aspects

Mathematical results are presented here for the classical (UM1-UM3) and quantum (UM4, UM5) standard map.

- UM1) **Anti-integrable limit.** A rigorous proof is given in the standard map for the existence of chaotic trajectories with unbounded momenta for large enough coupling constant $K > K_0$, where K_0 depends on a coding representation of a trajectory. The obtained chaotic trajectories correspond to stationary configurations of the Frenkel-Kontorova model with a finite (non-zero) photon gap. The concept of anti-integrability emerges from the theorems presented in [UM1].
- UM2) **Homoclinic tangencies.** The large basic sets, which fill in the torus as the parameter runs to infinity, are constructed. It is proven that, for a residual set of large parameters, these basic sets accumulated by elliptic periodic islands. It is shown there exists a $K_0 > 0$ and a dense set of parameters $K_0 \leq K < \infty$ for which the standard map exhibits homoclinic tangencies [UM2].
- UM3) **Hausdorff dimesion.** It is proven that stochastic sea of the standard map has full Hausdorff dimension for sufficiently large topologically generic parameters [UM3].
- UM4) **Proof of localization.** For the quantum standard map with a generic quadratic rotational spectrum the localization is proven for small kick amplitudes [UM4].
- UM5) **Quantum vs. classical out-of-time-ordered correlations.** For the quantum standard map it is shown that the correlations of quantum dynamical operators can decay not faster then an inverse square of time being in a drastic contrast with a possible exponential decay of correlations in the regime of full chaos. It is also shown that for Heisenberg operators depending on time there is no exponential instability in respect to operators at initial time (thus for operators the Kolmogorov-Sinai entropy is zero) [UM5]. The above analytical results for quantum correlations are confirmed in the numerical simulations [46]. The dependence of Heisenberg operators at time t in respect to operators at initial time, named as out-of-time-ordered correlators (OTOC), is also analyzed in more recent studies for the quantum standard map [UM6]. This approach finds extensions in OTOC studies of many-body quantum systems.

Physical aspects and numerical results

Results for the Ulam method for the standard map are presented in (UP1), Poincare recurrences in (UP2) and the fractal Weyl law for Perron-Frobenius operators in (UP3). Advanced numerical methods for the standard map are described in (UP4),(UP5). The results of the field theory for the quantum standard map are discussed in (UP6).

- UP1) **Ulam method for the standard map.** In 1960 Ulam proposed a method, known now as the Ulam method, for construction a finite size matrix approximate for the Perron-Frobenius operator of a dynamical system in a continuous phase space [UP1a]. The method allows to construct numerically a matrix of Markov transitions between cells in a discretized phase space with fully chaotic dynamics. The method is known to be converging to the continuous limit of Perron-Frobenius operator when the phase space is fully chaotic. However, for systems with a divided phase space an effective noise induced by a finite cell size breaks the convergence leading to a destruction of the invariant KAM curve. This problem was resolved in [UP1b] by a generalized Ulam method in which the Markov transitions between cells are generated by one chaotic trajectory starting inside a chaotic component. The extensive numerical studies based on the Arnoldi method show that the Ulam approximate of the Perron-Frobenius operator S (UPFO) on a chaotic component converges to a continuous limit. Typically, in this regime the spectrum of relaxation modes is characterized by a power law decay for small relaxation rates. The numerical results show that the exponent of this decay is approximately equal to the exponent of Poincare recurrences in such systems. The eigenmodes, or eigenstates, show links with trajectories sticking around stability islands. An example of such an eigenstate is shown in Fig.8U. The spectrum of UFPO S is shown in Fig.9U.

In [UP1c] it is shown that the Ulam method applied to dynamical symplectic maps, e.g. the standard map, generates Ulam networks which belong to the class of small-world networks appearing for social networks of people, actors, power grids, biological networks, and Facebook. The analysis of the small-world properties of Ulam networks on examples of the standard map and the Arnold cat map shows that the number

of degrees of separation, or the Erdös number, grows logarithmically with the network size for the regime of strong chaos. This growth is related to the Lyapunov instability of chaotic dynamics. The presence of stability islands leads to an algebraic growth of the Erdös number with the network size. The comparison of the time scales related with the Erdös number and the relaxation times of the Perron-Frobenius operator shows that they have a different behavior [UP1c].

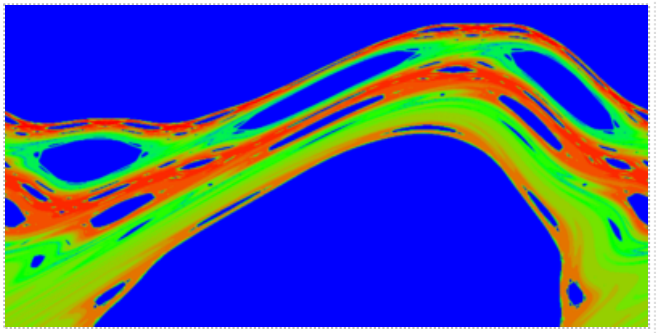

Figure 8: Fig. 8U. Amplitude of the eigenstate of the Ulam approximate of Perron-Frobenius operator of the standard map at $K = 0.971635406$; the number of cells and matrix size are $N_d = 127282$ and eigenvalue is $\lambda_2 = 0.99878108$; amplitude is proportional to color with maximum for red and zero for blue; upper part of phase plane is shown for the range $0 \le x/2\pi \le 1; 0 \le p/2\pi \le 0.5$.(from [UP1b])

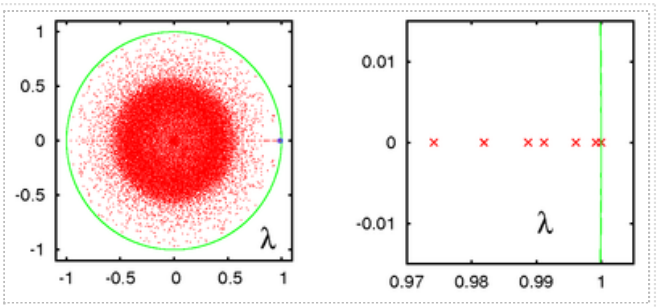

Figure 9: Fig. 9U. The complex plane of spectrum of eigenvalues λ of UFPO S of the standard map at $K = 0.971635406$; the number of cells and matrix size are $N_d = 16609$; right panel shows zoom of the global spectrum of left panel. (from [UP1b])

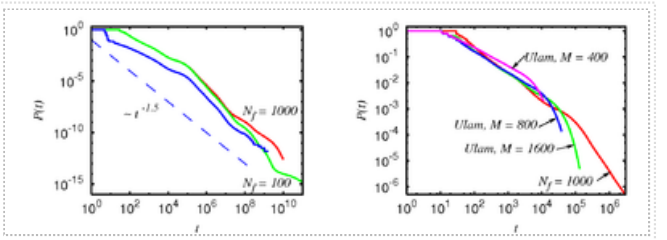

Figure 10: Fig. 10U. The left panel shows the statistics of Poincare recurrences $P(t)$ averaged over 10 random realizations and obtained by the survival Monte Carlo method proposed in [UP2a] operating here with $N_f = 1000$ surviving trajectories; magenta and red curves show independence of results on accuracy (overlapped curves), green curve shows data at $N_f = 100$ with larger fluctuations on large times t; blue curve shows data from [UP2b] at shorter times; the dashed line shows the slope $P \propto 1/t^{1.5}$. The right panel shows the results of red curve of left panel with the results obtained with the generalized Ulam method with the number of cells $M^2/2$ in the upper half plane of Fig.8U. (from [UP2a])

- UP2) **Algebraic Poincare recurrences.** The numerical studies of the Poincare recurrences in the standard map with the critical golden curve have been performed in [UP2a] with a new survival Monte Carlo method which allows to study recurrences on times changing by ten orders of magnitude (see Fig.10U). The comparison is done with the results of generalized Ulam method and localization properties of eigenstates of the Ulam matrix are analyzed. The recurrences at long times are determined by trajectory sticking in a vicinity of the critical golden curve and resonance structures. On the investigated scales the Poincare decay exponent, in $P \propto 1/t^{\alpha}$ is found to be approximately $\alpha \approx 1.58$ in a satisfactory agreement with early and more recent studies of various symplectic 2D maps [19], [20], [UP2c], [UP2d] thus indicating the universality of the exponent. The detailed theoretical explanation of the algebraic decay of Poincare recurrences and the exponent value is still lucking. It is interesting to add a few notes: A) in the standard map with dissipation (e.g. the right hand side of upper line Eq.(1) is multiplied by a coefficient less than unity) in the regime of a strange attractor the decay of Poincare recurrences is exponential [UP2c]; B) in the symplectic case additional noise leads to a diffusive type decay $P \propto 1/\sqrt{t}$ on a long time scale due to diffusion inside stability islands, when they are present [UP2c]; C) in the quantum standard map the quantum Poincare recurrences are characterized by a decay $P \propto 1/t$ due to quantum tunneling inside the stability islands [UP2e].
- UP3) **Fractal Weyl law.** For the standard map with absorption or dissipation in a chaotic regime it is show that the Ulam approximate of Perron-Frobenius operator is characterized by the fractal Weyl law with the exponent given by a half of the fractal dimension of related chaotic repeller or strange attractor [UP3a] (see also the section Ulam networks in Google matrix). The fractal Weyl law for the quantum standard map with absorption is analyzed in [44]. The semiclassical properties of eigenstates in quantum dissipative systems are analyzed in [UP3b],[UP3c].
- UP4) **Discretised standard map.** For many important Hamiltonian maps (e.g., the standard map) it is possible to construct related mappings that (i) carry a lattice into itself; (ii) approach the original map as the lattice spacing is decreased; (iii) can be iterated exactly using integer arithmetic; and (iv) are Hamiltonian themselves [UP4]. These lattice maps are compared to maps that use

floating-point arithmetic to evaluate the original map. The problems associated with roundoff error are analyzed and it is argued that lattice maps are superior to floating-point maps for the study of the long-term behaviour of Hamiltonian dynamical systems.

- UP5) **Visualization method.** A powerful visualization method for measure-preserving dynamical systems, based on frequency analysis and Koopman operator theory is applied to the standard map, and other maps, in [UP5].
- UP6) **Effects of noise for quantum localization.** The first numerical results reported in [46] showed that even a small noise in the kick amplitude ϵ can restore the diffusion in momentum with the rate being equal to its classical value. In [UP6] it was shonw that this noise of amplitude ϵ leads to the quantum diffusion with the coefficient $(\Delta n)^2/t = D_\epsilon \sim \epsilon^2 l^2 \sim \epsilon^2 k^4$. In fact noise destroys quantum coherence on a time scale $t_{coh} \sim 1/\epsilon^2$ after which a transition from one localized state to another one takes place leading to the above diffusion rate D_ϵ.
- UP7) **Field theory approach.** The field theory methods for the quantum standard map have been developed in [UP7]. It is shown that the effective theory describing the long wave length physics of the system is precisely the supersymmetric nonlinear sigma-model for quasi one-dimensional metallic wires. It is shown that the localization length is given by Eq.(4). This proves that the analogy between chaotic systems with dynamical localization and disordered metals can indeed be exact, as claimed by the authors. However, this approach misses certain properties of quantum evolution, thus it gives the finite localization length for the quantum kicked Harper model in the chaotic regime while the numerical results show the existence of delocalized quantum phase.

Related models and systems

Various models related to the standard map are discussed here: localization for the case of linear rotational spectrum (UR1), Shnirelman peak for level spacing statistics (UR2), studies of quantum synchronization (UR3), kicked rotator as a deterministic detector (UR4), effect of two interacting particles for two coupled kicked rotators (UR5), renormalization dynamical chaos for the critical spiral mean in the frequency modulated kicked rotator (UR6), effects of nonlinearity on localization in kicked rotator (UR7), fast Arnold diffusion, chaos measure and Poincare recurrences in coupled standard maps and many-body Hamiltonian systems (UR8), incommensurate extention of the standard map (UR9), Chirikov typical map (UR10) and universal features of the standard map (UR11).

- UR1) **Linear rotational phases.** The properties of quantum kicked rotator with rotational phases depending linearly on level number in Eq.(2) and generalized to any number of dimensions are considered in [UR1a],[UR1b], [UR1c]. The mathematical proof of localization of all eigenstates is given for small [UR1b] and arbitrary kick amplitudes [UR1c]. This result is rather clear from the view point of classical dynamics where linear dependence of Hamiltonian on actions (linear spectrum) leads to complete integrability of motion.
- UR2) **Shnirelman peak in level spacing statistics.** In 1975 Shnirelman proved the theorem about asymptotic multiplicity of Laplace operator [UR2a] which implies that the eigenenergies of generic integrable 2D billiards are exponentially quasidegenrate at large level numbers thus forming pairs of quasidegenerate levels forming the Shnirelman peak in the level spacing statistics. A physical interpretation of the Shnirelman theorem about such bulk quasidegeneracy is given in [UR2b]. Conditions for the strong impact of degeneracy on quantum level statistics are formulated allowing to extend the applications of the Shnirelman theorem to a broad class of quantum systems. It is shown that in some sense the degeneracy between the states connected by time-reversal symmetry is destroyed by tunneling between the future and the past (corresponding to a double well in momentum space). The numerical tests are done with the kicked rotator model of Eq.(2) with the modified potential $\cos\theta \to \cos\theta - 0.5\sin 2\theta$ so that the space symmetry is broken. The generic aspect of the Shnirelman peak is confirmed by the numerical results for rough billiards [UR2c].
- UR3) **Quantum synchronization.** The quantum standard map in infinite space x (kicked particle) is studied numerically [UR3a] by methods of quantum trajectories in presence of dissipation γ and applied static force f. The model allows to analyze the effects of quantum fluctuations on synchronization and establish the regimes where the synchronization is preserved in a quantum case (quantum synchronization). Thus at small values of dimensionless Planck constant $\hbar$ the classical devil's staircase remains robust with respect to quantum fluctuations while at large values synchronization plateaus are destroyed (see Fig.11U). Quantum synchronization in the model has close similarities with Shapiro steps in Josephson junctions [UR3b].

A dissipative quantum chaos is studied with the quantum trajectories approach applied to the quantum standard map with dissipation in [43]. For strong dissipation the quantum wave function in the phase space collapses onto a compact packet which follows classical chaotic dynamics and whose area is proportional to the Planck constant. At weak dissipation the exponential instability of quantum dynamics on the Ehrenfest time scale dominates and leads to wave packet explosion. The transition from collapse to explosion takes place when the dissipation time scale exceeds the Ehrenfest time. For integrable nonlinear dynamics the explosion practically disappears leaving place to collapse.

- UR4) **Deterministic detector and qubit sensor.** The properties of kicked rotator as a deterministic detector of qubit (spin or two state system) are analyzed in [UR4]. Th Hamiltonian of the whole system is a sum of kicker rotator Hamiltonian H_{kr}, qubit $H_s = \delta\sigma_x$ and coupling term $H_{int} = \epsilon_c \sigma_z \cos\theta \sum_m \delta(t-m)$. It is shown that in the regime of quantum chaos the detector acts as a chaotic bath inducing

qubit decoherence. The dependence of dephasing and relaxation rates on parameters is established. For a strong qubit-detector coupling the dephasing rate is given by the Lyapunov exponent of classical dynamics. For the strong coupling the detector performs an efficient measurement of qubit (see Fig.12U). In the case of weak coupling, due to chaos, the dynamical evolution of the detector is strongly sensitive to the state of the qubit. However, in this case it is unclear how to extract a signal from any measurement with a coarse-graining in the phase space on a size much larger than the Planck cell.

- UR5) **Two interacting kicked rotators.** The model of two kicked rotators with short range and finite range interactions in the momentum space is analyzed in [UR5a], [UR5b]. It is shown that the interaction leads to a strong enhancement of localization length. The case of interaction between two particles in higher effective dimensions is considered in [42]a) for the case of frequency modulated kicked rotators with two ($d_{eff} = 3$) and three ($d_{eff} = 4$) modulation frequencies. It is shown that in such models the interactions create delocalized pairs of particle in the regime when all one-particle states are exponentially localized. While without interactions the above models have been realized with cold atoms in kicked optical lattices (see [32] for the kicked rotator and [UR5c] for the case of two frequencies, described in more detail in UE4) below, the realization of local interactions in the momentum space is rather difficult for such systems.
- UR6) **Renormalization chaos.** The frequency modulated kicked rotator model was introduced in [46] for the quantum case. The corresponding classical volume preserving map has the form $\bar{y} = y - (k + \epsilon \cos z) \sin x$, $\bar{x} = x + \bar{y}$, $\bar{z} = x + 2\pi r_2$. The destruction of the spiral mean torus with the rotation numbers $r_1 = 1/\lambda^2$, $r_2 = 1/\lambda$, with $\lambda^3 - \lambda - 1 = 0$, $\lambda = 1.324718...$ is analyzed in [UR6a]. The critical torus exists along a critical curve in the plane (k, ϵ). In a certain interval of this curve the Greene residue dynamics with the renormalization time step is not universal indicating an emergence of dynamical renormalization chaos. Such a behaviour is strikingly different from the case of the critical golden curve in the standard map where the renormalization dynamics is universal corresponding to a fix point. Further analysis of critical tori in this map is reported in [UR6b]. An approximate renormalization-group transformation for Hamiltonian systems with three degrees of freedom is constructed in [UR6c].
- UR7) **Nonlinearity vs. localization.** The effects of nonlinearity on localization in kicked rotator (2) are analyzed in [UR7a] by adding after each kick a nonlinear phase shift of wavefunction amplitudes ψ_n in the momentum representation $\bar{\psi}_n = \exp(i\beta|\psi_n|^2)\psi_n$. The model was called the kicked nonlinear rotator (KNR). It is argued that there a certain critical strength of nonlinearity β_c below which the localization is essentially preserved, while for $\beta > \beta_c$ a subdiffusive spreading over momentum states n takes place in time with $n^2 \propto t^\alpha$ with the exponent $\alpha = 2/5$. The further numerical studies [UR7b] give a smaller value $\alpha = 0.35 \pm 0.03$ where the error bar is obtained from averaging over 10 realizations, taken from different rotation phases $n(n + \zeta)/2$ with $t \leq 10^8$; one realization with $t \leq 10^9$ has $\alpha = 0.35$ (the case of random rotational phases instead of $n(n + \xi)/2$ has the same exponent). In [UR7a] it was argued that KNR describes the nonlinear spreading over momentum harmonics in the kicked Gross-Pitaevskii equation on a ring $(0 \leq x < 2\pi)$ studied in [49]

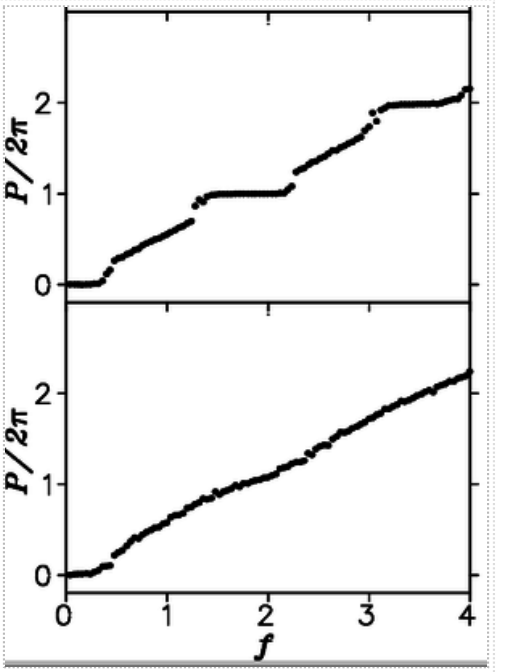

Figure 11: Fig. 11U. Quantum synchronization in the standard map with dissipation $\gamma = 0.25$ and static force f at $K = 0.8$; panels show the dependence of average momentum P on f for dimensionless Planck constant $\hbar = 0.05; 0.5$ for top; bottom panel. Top panel: synchronization remains stable in respect to quantum fluctuations; bottom panel: quantum fluctuations destroy synchronization. (from [UR3a])

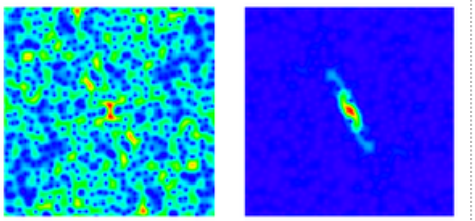

Figure 12: Fig. 12U. Standard map as a detector: Husimi function in action-angle variables $-\pi \leq p < \pi, 0 \leq x < 2\pi$ for qubit state up (left) and qubit state down (right) at $K = 4.5, \epsilon_c = 0.8, \delta = 0.1$, $\hbar = 0.0123$ at time $t = 20$. The initial states of kicked rotator and qubit (spin) are a Guassian packet centered at the fixed point $p = 0, x = \pi$ and spin state $(|0> + |1>)/\sqrt{2}$; color show density with blue for zero and red for maximum. (from [UR4])

$$i\hbar\frac{\partial\psi}{\partial t} = -\frac{1}{2}\frac{\partial^2\psi}{\partial^2 x} + \beta|\psi|^2\psi - k\cos x\ \psi\sum_{m=-\infty}^{\infty}\delta(t-mT)\ . \qquad (5)$$

This is confirmed in further numerical simulations [UR7c] with the numerically found exponent $\alpha \approx 0.4$ for $t \leq 10^7$. In [UR7c] the analogy between Kolmogorov energy flow from large to small spacial scales and conductivity in disordered solid state systems is proposed for model (5). It is argued that the Anderson localization can stop such an energy flow. The effects of nonlinear wave interactions on such a localization are analyzed. The results obtained for finite size systems show the existence of an effective chaos border between the Kolmogorov-Arnold-Moser (KAM) integrability at weak nonlinearity, when energy does not flow to small scales, and developed chaos regime emerging above this border with the Kolmogorov turbulent energy flow from large to small scales. Another conjecture, pushed forward in [UR7a], is that the destruction of Anderson localization in 1D disordered potential is characterized by the same subdiffusive spreading as for the KNR. This conjecture was confirmed in extensive numerical simulations with the discrete Anderson nonlinear Schrodinger equation (DANSE) (see [UR7c] and Refs. therein). A subdiffusive spreading of a Bose-Einstein condensate, with a repulsive interactions between atoms, had been observed in a disordered quasiperiodic lattice with a measured speading exponent $\alpha \approx 0.3 - 0.4$ [UR7d].

- UR8) **Fast Arnold diffusion.** The model of coupled standard maps with nearest left-right neighbour couplings K is used for investigations of classical chaos properties in many-body (or many dimensional) systems [UR8a],[UR8b]. This model is described by coupled standard maps

$$\bar{p_n} = p_n + (K/2\pi)[\sin(2\pi(x_n - x_{n-1})) + \sin(2\pi(x_n - x_{n+1}))], \quad \bar{x_n} = x_n + \bar{p_n}$$

  with $1 \leq n \leq N$ and periodic conditions in n.

In [UR8b] a skillful numerical method is used to compute the width of chaotic layers and Arnold diffusion rate inside the layer. The method is based on the computation of unstable fix points in high-dimensional phase space, and then determination of rotational period inside the layer via a certain number of trajectories [UR8b]. This approach allows to determine very small layer width $w_s \sim 10^{-22}$ and the related fast Arnold diffusion inside the layer $D \sim {w_s}^2 \sim 10^{-44}$ (see Fig.13U from [UR8b]). The main result obtained in [UR8b] is approximately algebraic (nonexponential) decay of the Arnold diffusion with a decrease of perturbation parameter K or increase of the related adiabaticity parameter $\lambda = 1/\sqrt{K}$. Certain explanations are proposed in [UR8b] but the origin of this slow decay of $D(\lambda)$ remains unclear. Further studies of this model [UR8c] show that at small coupling the measure of chaos is found to be proportional to the coupling strength with the typical maximal Lyapunov exponent being proportional to the square root of coupling. This strong chaos appears as a result of triplet resonances between nearby modes. The dynamics in such triplets remains chaotic even for $K \to 0$. In addition to strong chaos there is a weakly chaotic component having much smaller Lyapunov exponent, the measure of which drops approximately as a square of the coupling strength (K^2) down to smallest couplings reached. It is argued that this weak chaos is linked to the regime of fast Arnold diffusion discussed in [UR8b]. The investigation of Poincare recurrences in this model shows that their statistics is characterized by the algebraic decay $P \propto 1/t^\alpha$ with the Poincare exponent $\alpha \approx 1.3$ being independent of number of degrees of freedom [UR8d]. A conjecture is made about universal value of the Poincare exponent in systems with many degrees of freedom [UR8d]. A certain confirmation of this conjecture is given by the numerical results of Poincare recurrences in protein and DNA molecules where a similar value of the Poincare exponent is obtained from numerical simulations [UR8e],[UR8f]. Finally, the case of the many standard maps with a relatively strong kick amplitude K and weak couplings between all maps is considered in [UR8g]; the case of 4D coupled standard maps is studied in [UR8h]a) with approximate $\alpha \approx 1.6$ found; a similar model is studied in [UR8h]b) analyzing the influence of recurrence set choice.

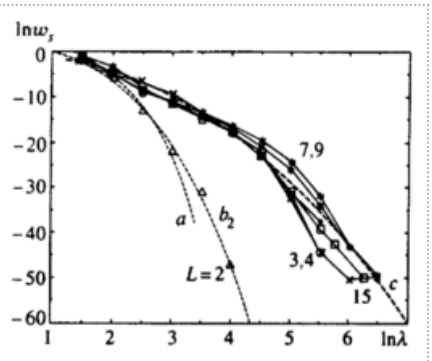

Figure 13: Fig. 13U. Dependence of chaotic layer width w_s on the adiabaticity parameter $\lambda = 1/\sqrt{K}$ is shown by broken solid lines connecting various symbols with resonance dimension $L = N$ indicated by numbers. The rate of Arnold diffusion inside chaotic layer is $D \sim {w_s}^2$. Data demonstrate nonexponential (approximately algebraic) decay of w_s on λ (from [UR8b] with more details given there).

- UR9) **Incommensurate standard map.** The incommensurate standard map is proposed and analysed in [UR9]. In difference from the standard map it has an additional harmonic (or two harmonics) in the kick equation for momentum having the form:

$$\bar{p} = p + K_1 \sin x + K_2 \sin \nu x \ , \ \bar{x} = x + \bar{p} \ , \tag{6}$$

where ν is an incommensurate irrational number (e.g. 0.618...). The critical curve in the plane (K_1, K_2) is found. Below this curve at small kick amplitudes, the dynamics is bounded by the isolating Kolmogorov-Arnold-Moser surfaces, whereas above a certain kick strength, it becomes unbounded and diffusive. The quantum evolution at small quantum kick amplitudes is somewhat similar to the case of the Aubry-André model studied in mathematics and experiments with cold atoms in a static incommensurate potential. It is shown that for the quantum map there is also a metal-insulator transition in space whereas in momentum we have localization similar to the case of two-dimensional Anderson localization. In the case of three incommensurate frequencies of the space potential, the quantum evolution is characterized by the Anderson transition similar to the three-dimensional case of the disordered potential. A similar map provides a description of comet and dark matter dynamics in planetary systems with two or more planets.

- UR10) **Chirikov typical map.** The typical map had been proposed and analyzed by Chirikov in 1969 [1]. The analytical expression for the Lyapunov exponent was derived in [UR10a] confirming the simple estimate given in [1] (see also [23]). The typical map is obtained from the standard map by a finite-number T of random phase-shift angles at each map iteration. The map has the form:

$$p_{t+1} = p_t + k \sin(x_t + \alpha_t) \ , \ x_{t+1} = x + p_{t+1} \ , \tag{7}$$

where independent random phase shifts α_t are uniformly distributed and are repeated periodically after T map iterations. The detailed study of classical and quantum map dynamics are reported in [UR10b]. The global chaos with unbounded diffusion appears for $k > k_c = \pi^2/(4T^{3/2})$ with $k_c << 1$ at $T >> 1$. Thus the typical map described a quasi-continuous chaotic flow. The Lyapunov exponent is $\lambda \approx 0.29k^{2/3}$ with the exact expression derived in [UR10a]. The diffusion rate in the regime of global chaos at $k > k_c$ is $D = p^2/t = k^2/2 \sim \lambda^3$. In the quantum case this diffusion is localized due to quantum interference effects (similar to the Anderson localization in disordered solid-state systems) with the localization length $\ell = k^2T/(2\hbar^2)$ where $\hbar$ is the dimensionless Planck constant [UR10b]. The Ehrenfest time scale in this system is $t_E \approx \ln(2\pi/\sqrt{\hbar})/\lambda$ [UR10b]. The exponentially fast spearing of initial wave packet of coherent state is illustrated in [UR10b] (Fig.4 there).

- UR11) **Universality of the standard map.** A variety of two-dimensional symplectic maps can be reduced locally to the standard map which corresponds to a local constant density of resonances. As an example of such physical systems we note the Microwave ionization of hydrogen atoms and dark matter dynamics in the Solar System desribed by the Kepler map. Other examples correspond to a dynamics inside a narrow separatrix chaotic layer [19], dust dynamics around rotating binary [UR11a], Wigner crystal in a periodic potential [UR11b] and many other systems.

Experimental realizations

Various experiments with systems related to the standard map are described here including cold atom experiments with phase modulated effective pendulum (UE1), high-order quantum resonances observed with BEC and noncondensed cold atoms (UE2), time reversal of BEC atomic waves in quantum chaos regime (UE3), cold atom experiments with frequency modulated kicked rotator and observation of Anderson transition (UE4), realizations of kicked rotator with molecules in pulsed laser field (UE5), observation of the Aubry transition for cold ions in optical periodic lattice and thermoelectric properties of this system (UE6), stabilization theory of electron edge states in magnetic and microwave fields and its experimental observation(UE7).

- UE1) **Phase modulated pendulum.** The classical dynamics of phase modulated pendulum, described by the rescaled dimensionless Hamiltonian $H = p^2/2 - k\cos(\phi - \lambda \sin t)$ is analyzed in [1],[10]. In the regime of fast resonance crossing $k/\lambda > 1, \lambda \gg 1$ the dynamics is approximately described by the standard map since each crossing gives a kick to momentum of particle. The chaos region is restricted to $|p| < \lambda$ since the crossing is possible only in this region. From the map the chaos border is $k > 0.04\sqrt{\lambda}$ with a diffusion rate $D \approx k^2/\lambda$. The quantum case [UE1a] is characterized by an effective dimensionless Planck constant $\hbar_{eff}$ with the dynamical localization length $\ell = \pi D/{\hbar_{eff}}^2$. Thus in the classical case the fluctuations of momentum (or average populated number of quantum states Δn) grow linearly with λ while in the quantum case at they drops at large λ as $\Delta n \approx \ell \propto D \propto 1/\lambda$ (see Fig.14U). It is argued that this model describes the quantum dynamics of Josephson junctions at small dissipation. In [UE1b] it is shown that the same Hamiltonian describes cold atoms in a modulated standing light wave. This physical system happens to be more accessible for experimental realization and the dynamical localization of quantum chaos in an effective modulated pendulum is observed by Raizen group in [UE1c].
- UE2) **Kicked rotator with cold atoms.** After the realization of kicked rotator with cold atoms by Raizen group [32] the properties of this model have been studied by different experimental groups. Thus the high-order quantum resonances predicted in [28]a) are observed with BEC [UE2a] and noncondensed cold atoms [UE2b]. The cold atom experiments with a kicked rotator (particle) under an applied static field

are discussed at the article Kicked cold atoms in gravity field.

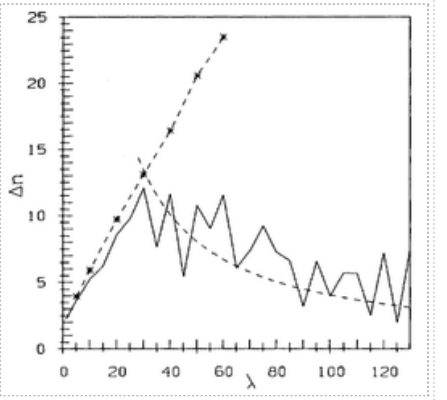

Figure 14: Fig. 14U. Root mean square of occupied levels Δn in modulated quantum pendulum versus the normalized modulation amplitude λ at $k = 15$, $\hbar_{eff} = 1.58$; classical results are shown by stars connected by dashed lines, quantum results are shown by full curve and the quantum localization theory is shown by dashed curve. (from [UE1a], this Fig. is also used in [UE1b]).

- UE3) **Boltzmann-Loschmidt dispute realization with cold atoms.** The famous dispute between Boltzmann [UE3a] and Loschmidt [UE3b] on time reversal of moving atoms (see also [45]) remained without any experimental verification from 1876 till recently since it is rather hard to invert time for matter waves. The method for realization of time reversal of atomic waves and BEC has been proposed for cold atoms [48] and BEC [UE3c] moving in kicked optical lattice in the regime of quantum chaos for kicked rotator. This is reached by propagating the evolution described by (2) or (5) during time t_r at $T = 4\pi + \epsilon$ and then replacing the kick period $T \to 4\pi - \epsilon$ and displacing the lattice in x by π (see (5)) that generates an approximate time reversal of atoms with small initial momentum at time $2t_r$. This theoretical proposal is realized experimentally with BEC of Rb atoms [UE3d] with the time reversal after $t_r = 5$ kicks and return time $2t_r = 10$, as it is shown in Fig.15U. Even if the classical dynamics of this model is deeply in the chaotic regime with $K \approx 22$ the quantum system returns close to the initial distribution. Of course, if would be desirable to increase t_r by a factor 10 to 20 with a larger kick amplitude $k \sim 10$ so that after such a time the classical trajectories simulated on a computer would not return to the origin (see Fig.7) in contrast to the quantum evolution (see Fig.6). It is possible to hope that this first experimental test for the Bolzmann-Loschmidt dispute will be extended to the above parameters to understand in a better manner the properties of time reversal for dynamics of classical and quantum chaotic atomic motion.
- UE4) **Anderson transition in effective dimensions.** The frequency modulated kicked rotator is introduced in [46]. It is described by the Hamiltonian $H = Tn^2/2 + k(1 + \epsilon\Pi_{m=1}^{n_f}\cos(\omega_m t))\cos\theta\delta_p(t-1)$, where $n = -i\partial/\partial\theta$ and $T = \hbar$ plays the role of effective Plank constant; $\delta_p(t-1)$ is periodic delta-function of unit period and Π notes the product. Since the phases $\theta_m = \omega_m t$ evolve linearly with time it is possible to go to extended phase space with additional actions $n_m = -i\partial/\partial\theta_m$ so that the system will have the effective dimension $d_{eff} = n_f + 1$. The frequencies ω_m are incommensurate between themselves and 2π. Thus the case with $d_{eff} = 2$ is studied in [46] showing that the number of excited levels is growing exponentially with $\epsilon, k = K/T = K/\hbar$ (see Fig.9 in [46]) corresponding to Anderson localization in two dimensions. The case of $d_{eff} = 3, 4$ is studied in [42]a) , [UE4a] (the case of random phases is considered there instead of $Tn^2/2$) showing that there is the Anderson transition from exponential localization of probability distribution over levels to a diffusive spreading over them above a certain delocalization border for k at given $\epsilon > 0$. Thus the critical values are $k_c \approx 1.8$ at $\epsilon = 0.75, d_{eff} = 3$ and $k_c \approx 1.15$ at $\epsilon = 0.9, d_{eff} = 4$ [42]a). The critical exponents ν for the localization length and s diffusion rate in the vicinity of critical point are found to be $\nu = 1.537 \pm 0.0539; s = 1.583 \pm 0.0511$ for $d_{eff} = 3$ and $\nu = 1.017 \pm 0.041; s = 2.003 \pm 0.074$ for $d_{eff} = 4$ [UE4a]. These values are in agreement with the renormalization theory for Anderson transition and the relation $s = (d-2)\nu$ [UE4a]. The results obtained in [42]a) , [46] attracted interest of cold atom experimental groups. The model with $d_{eff} = 3$ is studied experimentally by Garreau group [UR5c] with cold cesium atoms finding the transition at $k = K/T \approx 1.88$ at $\epsilon = 0.75, T = \hbar = 2.89$ being in agreement with numerical simulations and the above value found in [42]a) (the difference in the rotational phases is not very important since for quadratic rotational phases the classical chaos border $K \approx 0.3$ established in [UR6a] is much below the Anderson critical point). The Garreau group experiments [UR5c], [UE4b] succeeded to obtain experimentally the critical exponents in a vicinity of 3D Anderson transition that is strikingly exceptional and was never realized in the solid state experiments. The overview of the Garreau group experiments is given in [UE4b]. The experiments for 2D case demonstrated exponential growth of the localization length confirming the early results obtained in [46] (Fig.9 there). Since the numerical simulations of the frequency modulated kicked rotator are very efficient (evolution takes place only in one dimension) this model and its extensions are investigated with various physical effects including quantum Hall effect in two dimensions [UE4c], metallic phase of the quantum Hall in four dimensions with computations of critical exponents [UE4d], topological quantum phenomena with spin-half quasiperiodic quantum kicked rotators [UE4e]. However, an experimental realization of these models with cold atoms is challenging. The frequency modulated kicked rotator with up to 10 frequencies is studied numerically in [UE4f], the critical exponent for the diffusion rate in the critical point vicinity is found to be in agreement with the results of renormalization theory, however, certain deviations are found for the exponent in the localization phase at large dimensions, even if this can be related to a restricted computation times since large localization length requires times $t_{comp} \gg l^{d_{eff}}$.
- UE5) **Kicked rotator with molecules.** The kicked rotator model is realized with nitrogen molecules kicked by a periodic train of

femtosecond laser pulses [UE5a], [UE5b], [UE5c]. These experiments allows to realize about 15 kicks with up to 25 rotational states. These experiments demonstrated the effects of quantum resonance and dynamical localization of quantum chaos.

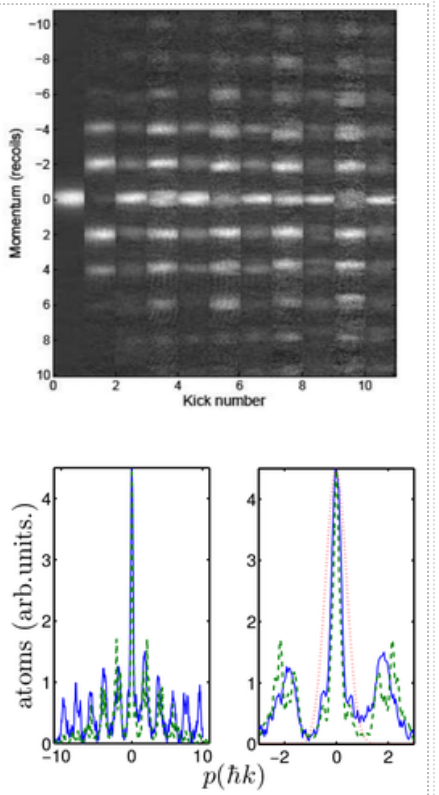

Figure 15: Fig. 15U. Time reversal of Bose-Einstein condensate of Rb cold atoms in the regime of quantum chaos fo**Renormalization chaos.**r $\epsilon = 1, k = K/T \approx 2$ (see text); top panel shows probability distribution in momentum (expressed in recoil units) after each kick; the reversal time is $t_r = 5$; the bottom left panel shows the distribution at the return moment $2t_r = 10$ (experimental data are shown by the solid blue curve, numerical simulations by the dashed green curve) and the right panel shows zoom of the left panel with initial distribution shown by dashed red curve. (from [UE3d]).

- UE6) **Wigner crystal thermoelectricity.** It is shown in [53] that a Wigner crystal of cold ions placed in a periodic optical lattice potential has the Aubry transition when the potential amplitude K becomes larger than a certain critical value K_c (measured in units of Coulomb interaction strength on a unit length at period 2π). This system is locally described by the Frenkel-Kontorova model and corresponding standard map with the chaos border parameter $K_{eff} = 0.5K_c(2\pi/\nu)^3 \approx 1$,where ν is the charge density per period. Thus for a given density the Aubry transition takes place at $K_c \approx 0.034(\nu/\nu_g)^3$ where for the golden mean density $\nu_g = 1.618...$ the numerics gives a more exact, but close, value $K_c = 0.0462$ [53]. Below K_c the ion chain can easily slide while above the transition it is pinned by the potential. This strongly affects the friction of ion chain and in this way the signatures of Aubry transition are observed with cold Yb ions by the Vuletic group [UE6a], even if the number of ions remains small, only up to 5, due to experimental restrictions. Other groups start to observe signatures of Aubry transition with tens of ions [UE6b]. The properties of this system are rather nontrivial and their theoretical and experimental investigations are important for understanding of physics of friction on nanoscale as discussed in [UE6c]. It is striking that in the Aubry phase the system has remarkable thermoelectric properties with large values of Seebeck coefficient and such high figure of merit values as $ZT \approx 4$ [UE6d] (see Fig.16U). Even $ZT \approx 8$ can be reached in numerical simulations at lower electron (or ion) density [UE6e]. Thus it is rather plausible that this model will allow to understand the main physical features of thermoelectricity which foundations have been done by Ioffe in far 1957 [UE6f]. Due to important technological applications of thermoelectric materials with high figure of merit various materials are actively investigated with first-principles calculations (see e.g, [UE6g]). However, according to [53] the quantum properties of this system are rather nontrivial, being similar to a dynamical version of spin glass systems with a huge quasi-degeneracy in the ground state vicinity, and hence it remains questionable if these first-principle calculations are able to describe correctly thermoelectricity in the quantum Aubry phase.
- UE7) **Microwave stabilization of electron edge transport.** For two-dimensional electron gas in a perpendicular magnetic field it is shown that a microwave field leads to stabilization of edge trajectories leading to their long distance propagation [UE7a]. The dynamics of propagation is approximately described by the standard map wher the stabilization takes place due to trapping of orbits inside the main resonance in presence of noise and dissipation (see Fig.17U). The signatures of this stabilization are observed with 2DEG high mobility samples in experiments reported in [UE7b].

Fundamental aspects of chaos and open problems

Fyndamental aspects of classical and quantum chaos and related open problems are discussed here.

- UF1) **Ehrenfest time scale and correspondence principle.** The Bohr correspondence principle [UF1a] tells that the quantum evolution should reproduce the classical evolution in the limit of small values of effective dimensionless Planck constant $\hbar$ (or related high quantum numbers $n_q \sim 1/\hbar$). The Ehrenfest theorem [UF1b] guarantees that the classical variables remain close to the averages of quantum operators during time scale t_E on which the quantum wave packet remains well localized in coordinate and momentum space. Usually the case of initial coherent wave packet is considered. For integrable dynamics the separation of different trajectories in the phase space increases polynomially in time (e.g. linearly in time for a ballistic free propagation). Thus for such integrable dynamics the classical and quantum correspondence remains valid till rather large time scale $t_E = t_{int} \sim O(1/\hbar^\nu), \nu \sim 1$. This is fully in agreement with the Bohr correspondence principle. The situation is changed drastically for the case of chaotic dynamics. Here the classical trajectories are diverging

exponentially in time due to exponential instability of motion and positive Kolmogorov-Sinai entropy h so that generally we have $\Delta x(t) \sim \exp(ht)\Delta x(t=0)$. Due to this instability of motion the initial coherent wave packet with $\Delta x(t=0) \sim \sqrt{\hbar}$ chaotically spreads over the whole accessible phase space (e.g. 2π in coordinate axis for the standard map) after the logarithmically short Ehrenfest time scale $t_E \approx (\ln(1/\hbar))/2h$ [23] (the term Ehrenfest time scale was coined in [24]). In [UM5] it was shown that the quantum correlations (or as they say now OTOC, see point UM5 above) cannot decay exponentially with time, in contrast to exponentially decaying classical correlations. Thus after the Ehrenfest time scale $t_E \approx (\ln(1/\hbar))/2h \sim 1$ the correspondence principle is not working for these correlations. This result is confirmed in the numerical simulations with the quantum standard map in [46] (see Table 1 and Fig.2 there): the quantum correlations stop to decay after reaching the level of quantum fluctuations being of the order of $\hbar$. However, since the value of these correlations is relatively small they affect the diffusive growth of energy only after much larger time scale $t_D \sim 1/\hbar^2$ [23],[UM5], [UF1c],[46],[24]. It should be noted that an early attempt to determine the correspondence time between quantum operator averages and related classical averages was done in [UF4]; there the quantum averages were expendened in series of Planck constant finding that the quantum corrections are growing exponentially with time. However, the quantum operator average and its expansion was compared in [UF1d] with the classical value obtained from only one classical trajectory from the packet centre while for a correct comparison one needs to compare with the average over the initial Liouville function (distribution of trajectories) corresponding to the initial quantum wave packet. Indeed, due to exponential divergence of trajectories the average over Liouville fnuntion becomes on logarithmic times very different from the result given by the trajectory from the initial packet centre even in the case of purely classical dynamics. Due to this reason the results of [UF1d] are not conclusive and tell not much about the Ehrenfest time scale.

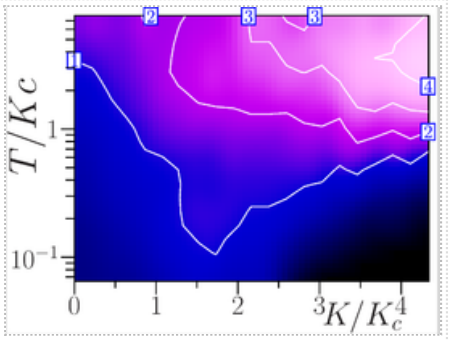

Figure 16: Fig. 16U. Dependence of ZT figure of merit of Wigner crystal in a periodic potential on parameters rescaled temperature T/K_c and periodic potential amplitude K/K_c with K_c being the critical amplitude at Aubry transition; ZT is proportional to color (red for maximum, blue for zero; contour curves show ZT values). (from [UE6d]).

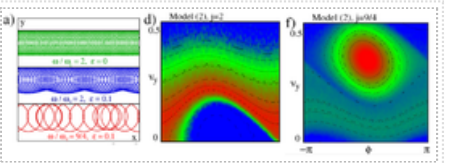

Figure 17: Fig. 17U. Microwave stabilization of edge transport. a) Examples of electron trajectories along sample edge for several ratios of microwave frequency to cyclotron frequency $j = \omega/\omega_c$ and dimensionless field strength ϵ being perpendicular to the edge (y −axis). d),f) Density of propagating particles on the phase plane of velocity edge perpendicular component and microwave phase at the edge collision moment; simulations with the Chirikov standard map with noise and dissipation; red/blue marks maximal/zero density. For $j = 2$ in d) trajectories are escape rapidly from the edge to the sample bulk with density maximum at separatrix, For $j = 9/4$ in f) trajectories are trapped inside the main resonance corresponding to stabilization of propagation along the edge (from [UE7a]).

- UF2) **Mathematical prove of localization in the quantum standard map at finite kick amplitudes.** The mathematical prove of localization for the quantum standard map exists only for the limit of small kick amplitudes (see [UM4] and related point UM4). Its extension for finite and large kick amplitudes represents an open problem.
- UF3) **Mathematical prove of positive measure of chaos in the standard map.** Till present there is no mathematical prove if the measure of chaotic component for the classical dynamics of the standard map is positive at least for some values of parameter K. The related mathematical results are described in points UM1,UM2,UM3 but the prove for chaos measure is still absent.
- UF4) **Algebraic Poincare recurrences.** The problem of algebraic decay of Poincare recurrences and correlations still waits its solution (see point UP2). The numerical results give the algebraic decay exponent $\alpha \approx 1.5$ with a decay $P(\tau) \propto 1/\tau^{\alpha}$. Even if the numerical studies allow to reach rather high times $\tau \sim 10^{10}$ the asymptotic behavior of decay is still in question. Different semi-analytical estimates and models for trajectories trapping near integrable islands had been proposed in [19],[UP2d], [UF4a] but still there is no detailed analytical theory for the algebraic Poincare recurrences. Their decay in higher dimensions also remains an open problem [UR8d].
- UF5) **Dynamical renormalization chaos.** The renormalization transformation operation can be considered as a dynamical propagation in discrete time corresponding to one iteration. Then an example of critical golden curve of the standard map, considered in [3],[4],[5], can be viewed as a fixed point or simple point repeller (attractor at a critical parameter). A critical invariant curve with a random coefficients in the continued fraction expansion of its rotation number (e.g. only 1 and 2 values) can be viewed as an example of a random renormalization dynamics under an external noise [19]. It is possible to expect that the randomness can also appear not due to external origin (linked to the fraction expansion coefficients) but due to a dynamics of the renormalization steps. The indications for such a dynamical renormalization

chaos are discussed in [UR6a],[UR6b] for the critical spiral mean surface (see point UR6). However, more detailed analysis of this problem requieres further studies.

- UF6) **Measure of chaos in many-body systems at weak perturbation.** In [UR8c] it is shown that the chaos measure in the model of coupled standard maps decreases proportionally to perturbation as $\mu_{ch} \sim KN$ with a typical maximal Lyapunov exponent $\lambda \sim \sqrt{K}$ (see point UR8). The origin of such a dependence is related to presence of triple resonances with the same frequencies when the chaos survives at arbitrary small perturbation since the KAM theory is not applicable in such a case (similar situation was discussed for classical massive color Yang-Mills fields in [UF6a]). However such a triple resonance does not lead to a global Arnold diffusion appearing in chaotic separatrix layers and analyzed in [UR8b] with an approximate dependence $D \sim K^{6.5} \sim K^{3/2} w_s^2$, where $w_s \sim K^{2.5}$ is a chaos measure for an individual chaotic separatrix layer at given K. The results presented in [UR8c] indicate emergence of slow chaos in such separatrix layers with much smaller Lyapunov exponents $\lambda_s \ll \lambda \sim \sqrt{K}$. The total measure of such slow chaos in all separatrix layers is estimated to scale as $w_{sch} \sim K^{1.6}$ that approximately in argeement with the dependence $D \sim K^{6.5}$ (see discussion in [UR8c]). However, it is clear that the question about the measure and diffusion over chaotic separatrix layers in many-body systems at small pertirbations requires further investigations.
- UF7) **Destruction of Anderson localization by weak nonlinearity.** As discussed in point UR7 a weak nonlinearity leads to a destruction of Anderson localization in disordered lattices and subdiffusive spreading with the spreading exponent $\alpha \approx 0.3 - 0.4$ [UR7a],[UF7a]. The spearing continues up to the highest reached dimensionless times $t_s \approx 10^8$ for the discrete Anderson nonlinear Schrodinger equation (DANSE) [UF7a], $t_s \approx 10^9$ for the nonlinear kicked rotator [UR7a],[UR7b],[UR7c]. Similar values of the spreading exponent are reported for a better disorder averaging and other 1D lattices with nonlinearity [UF7b],[UF7c]. A discrete-time nolinear lattice map allowed to reach times $t_s \approx 10^{12}$ (for one disorder realization) with approximately the same exponent $\alpha \approx 0.33$ [UF7d]. These results demonstrate a universal nature of destruction of Anderson localization by a weak or moderate nonlinearity. The main surprize of this effect is that with the increasing size Δn of the wave packet the local strength of nonlinearity goes to zero. In [UR7a] it is argued that the nonlinear frequency width is descreasing as $\beta/\Delta n$ that is comparable with the frequency uncertainty resolution $\delta\omega \sim 1/\Delta n$ for $\beta > \beta_c \sim 1$. Thus the discrete nature of the spectrum is not resolved at large times for $\beta > \beta_c$. However, the deeper understanding of physical mechanisms behind such an unlimited speading requires a profound analysis of properties of many-body chaos in the limit of very weak nonlinearity as discussed in points UR7, UR8, UF6. In 2D DANSE model the spearing exponent is found to be $\alpha \approx 0.24$ [UF7e].

References added after 2008

[UM1] S.Aubry, G.Abramovici, "Chaotic trajectories in the standard map. The concept of anti-integrability", Physica D 43: 199 (1990).

[UM2] P.Duarte, "Plenty of elliptic islands for the standard family of area preserving maps", Annales de l'I.H.P. Sec. C 11(4): 359 (1994).

[UM3] A.Gorodentski, "On stochastic sea of the standard map", Comm. Math. Phys. 309(1): 155 (2012).

[UM4] J.Bourgain, "Estimates on Green's functions, localization and the quantum kicked rotor model", Ann. Math. 156: 249 (2002).

[UM5] D.L.Shepelyanskii, "Dynamical stochasticity in nonlinear quantum systems", Teor. Math. Fiz. 49: 117 (1981) (in Russian); Theor. Math. Phys. 49(1): 925 (1981) (English trans.); Preprint INP 80-157, dated June 30, Novosibirsk (1980).

[UM6] R.Hamazaki, K.Fujimoto, M.Ueda, "Operator noncommutativity and irreversibility in quantum chaos", arXiv:1807.02360[cond-mat.stat-mech] (2018)

[UP1a] S.M.Ulam, "A Collection of mathematical problems, Interscience tracts in pure and applied mathematics", Interscience, New York 8: 73 (1960).

[UP1b] K.M.Frahm, D.L.Shepelyansky, "Ulam method for the Chirikov standard map", Eur. Phys. J. B 76: 57 (2010).

[UP1c] K.M.Frahm, D.L.Shepelyansky, "Small world of Ulam networks for chaotic Hamiltonian systems", Phys. Rev. E 98: 032205 (2018).

[UP2a] K.M.Frahm, D.L.Shepelyansky, "Poincare recurrences and Ulam method for the Chirikov standard map", Eur. Phys. J. B 86: 322 (2013).

[UP2b] M.Weissm L.Hufnagel, R.Ketzmerick, "Universal power-law decay in Hamiltonian systems?", Phys. Rev. Lett. 100: 184101 (2008).

[UP2c] B.V.Chirikov, D.L.Shepelyansky, "Correlation properties of dynamical chaos in Hamiltonian systems", Physica D 13: 395 (1984), [24] (http://www.quantware.ups-tlse.fr/dima/myrefs/my018.pdf) , detailed BINP preprint in Russian [25] (http://www.quantware.ups-tlse.fr/dima/myrefs/my018binp.pdf)

[UP2d] G.Cristadoro, R.Ketzmerick, "Universality of algebraic decays in Hamiltonian systems", Phys. Rev. Lett. 100: 184191 (2008).

[UP2e] G.Casati, G.Maspero, D.L.Shepelyansky, "Quantum Poincare recurrences", Phys. Rev. Lett. 82: 524 (1999).

[UP3a] L.Ermann, D.L.Shepelyansky, "Ulam method and fractal Weyl law for Perron-Frobenius operators", Eur. J. B 75: 299 (2010).

[UP3b] G.G.Carlo, L.Ermann, A.M.F.Rivas, M.E.Spina, "Classical properties of the leading eigenstates of quantum dissipative systems", arXiv:1705.03847(quant-ph) (2017).

[UP3c] G.G.Carlo, L.Ermann, A.M.F.Rivas, M.E.Spina, D.Poletti "Classical counterparts of quantum attractors in generic dissipative systems", Phys. Rev. E 95: 062202 (2017).

[UP4] D.J.D. Earn, S.Tremaine, "Exact numerical studies of Hamiltonian maps: Iterating without roundoff error", Physica D 56: 1 (1992).

[UP5] Z.Levnajic, I.Mezic, "Ergodic theory and visualization. II. Fourier mesochronic plots visualize (quasi)periodic sets", Chaos 25: 053105 (2015).

[UP6] E.Ott, T.M.Antonsen Jr., J.D.Hanson, "Effect of noise on time-dependent quantum chaos", Phys. Rev. Lett. 53: 42187 (1984).

[UP7] A.Altland, M.Zinbauer, "Field theory of the quantum kicked rotor", Phys. Rev. Lett. 77: 4536 (1996).

[UR1a] S.Fishman, D.R.Grenpel, R.E.Prange, "Localization in an incommensurate potential: an exactly solvable model", Phys. Rev. Lett. 49: 833 (1982).

[UR1b] J.Bellissard, R.Lima, E.Scoppola, "Localization in v-dimensional incommensurate structures", Comm. Math. Phys. 88: 465 (1983).

[UR1c] A.L.Figotin, L.A.Pastur, "An exactly solvable model of a multidimensional incommensurate structure localization for linear spectrum", Comm. Math. Phys. 95: 401 (1984).

[UR2a] A.I.Shnirelman, "On asymptotic multiplicity of spectrum of Laplace operator", Usp. Mat. Nauk 30: 265 (1975) (in Russian); A.I.Shnirelman, addendum in V.F.Lazutkin, "KAM Theory and semiclassical approximations of eigenfunctions, Springer, Berlin (1993).

[UR2b] B.V.Chirikov, D.L.Shepelyansky, "Shnirelman peak in level spacing statistics", Phys. Rev. Lett. 74: 518 (1995), [26] (http://www.quantware.ups-tlse.fr/dima/myrefs/my070.pdf)

[UR2c] K.M.Frahm, D.L.Shepelyansky, "Quantum localization in rough billiards", Phys. Rev. Lett. 78: 1440 (1997).

[UR3a] O.V.Zhirov, D.L.Shepelyansky, "Quantum synchronization", Eur. Phys. J. D 38: 375 (2006).

[UR3b] S.Shapiro, "Josephson currents in superconducting tunneling: the effect of microwaves and other observations", Phys. Rev. Lett. 11: 80 (1963).

[UR4] J.W.Lee, A.V.Averin, G.Benenti, D.L.Shepelyansky, "Model of a deterministic detector and dynamical decoherence", Phys. Rev. A 72: 012310 (2005).

[UR5a] D.L.Shepelyansky, "Coherent propagation of two interacting particles in a random potential", Phys. Rev. Lett. 73: 2607 (1994).

[UR5b] F.Borgonovi, D.L.Shepelyansky, "Enhancement of localization length for two interacting kicked rotators", Nonlinearity 8: 877 (1995).

[UR5c] J.Chabe, G.Lemarie, B.Gremaud, D.Delande, P.Szirftgiser, J.C.Garreau, "Experimental observation of the Anderson metal-insulator transition with atomic matter waves", Phys. Rev. Lett. 101: 255702 (2008).

[UR6a] R.Artuso, G.Casati, D.L.Shepelyansky, "Break-up of the spiral mean torus in a volume-preserving map", Chaos, Solitons & Fractals 2(2): 181 (1992).

[UR6b] A.M.Fox, J.D.Meiss, "Greene's residue criterion for the breakup of invariant tori of volume-preserving maps", Physica D 243(1): 45 (2013).

[UR6c] C.Chandre, H.R.Jauslin, G.Benfatto, A.Celletti, "Approximate renormalization-group transformation for Hamiltonian systems with three degrees of freedom", Phys. Rev. E 60: 5412 (1999).

[UR7a] D.L.Shepelyansky, "Delocalization of quantum chaos by weak nonlinearity", Phys. Rev. Lett. 70: 1787 (1993).

[UR7b] L.Ermann, D.L.Shepelyansky, "Destruction of Anderson localization by nonlinearity in kicked rotator at different effective dimensions", J. Phys. A: Math. Theor. 47: 335101 (2014).

[UR7c] D.L.Shepelyansky, "Kolmogorov turbulence, Anderson localization and KAM integrability", Eur. Phys. J. B 85: 199 (2012).

[UR7d] E.Lucioni, B.Deissler, L.Tanzi, G.Roati, M.Zaccanti, M.Modugno, M.Larcher, F.Dalfovo, M.Inguscio, G.Modugno, "Observation of subdiffusion in a disordered interacting system", Phys. Rev. Lett. 106: 230403 (2011).

[UR8a] K.Kaneko, T.Konishi, "Diffusion in Hamiltonian dynamical systems with many degrees of freedom", Phys. Rev. A 40(10): 6130 (1989).

[UR8b] B.V.Chirikov, V.V.Vecheslavov, "Arnold diffusion in large systems", JETP 85(3): 616 (1997) (Zh. Eksp. Teor. Fiz. 112: 1132 (1997), [27] (http://www.quantware.ups-tlse.fr/chirikov/refs/chi1997.pdf)

[UR8c] M.Mulansky, K.Ahnert, A.Pikovsky, D.L.Shepelyansky, "Strong and weak chaos in weakly nonintegrable many-body Hamiltonian systems", J. Stat. Phys. 145: 1256 (2011).

[UR8d] D.L.Shepelyansky, "Poincare recurrences in Hamiltonian systems with a few degrees of freedom", Phys. Rev. E 82: 055202(R) (2010).

[UR8e] D.E.Shaw, P.Maragakis, K.Lindorff-Larsen, S.Piana, R.O.Dror, M.P.Eastwood, J.A.Bank, J.M. Jumper, J.K.Salmon, Y.Shan, W.Wriggers, "Atomic-level characterization of the structural dynamics of proteins", Science 330: 341 (2010).

[UR8f] A.K.Mazur, D.L.Shepelyansky, "Algebraic statistics of Poincare recurrences in a DNA molecule", Phys. Rev. Lett. 115: 188104 (2015).

[UR8g] E.G.Altmann, H.Kantz, "Hypothesis of strong chaos and anomalous diffusion in coupled symplectic maps", EPL 78: 10008 (2007).

[UR8h] a) S.Lange, A.Backer, R.Ketzmerick, "What is the mechanism of power-law distributed Poincaré recurrences in higher-dimensional systems?", EPL 116: 30002 (2016); b) M.Sala, R.Artuso, C.Manchein, "Anomalous dynamics and the choice of Poincare recurrence set", Phys. Rev. E 94: 052222 (2016).

[UR9] L.Ermann, D.L.Shepelyansky, "Incommensurate standard map", Phys. Rev. E 80: 016210 (2009).

[U10a] A.B.Rechester, M.N.Rosenbluth, R. B. White, "Calculation of the Kolmogorov entropy for motion along a stochastic magnetic field", Phys. Rev. Lett. 42: 1247 (1979).

[UR10b] K.M.Frahm, D.L.Shepelyansky, "Diffusion and localization for the Chirikov typical map", Phys. Rev. E 99: 012215 (2019).

[UR11a] J.Lages, D.L.Shepelyansky, I.I.Shevchenko, "Chaotic zones around cosmic spinning minor bodies", Astronomical Journal 153: 272 (2017).

[UR11b] O.V.Zhirov, J.Lages, D.L.Shepelyansky, "Thermoelectricity of cold ions in optical lattices", Eur. Phys. J. D 73: 148 (2019).

[UE1a] R.Graham, M.Schlautmann, D.L.Shepelyansky, "Dynamical localization in Josephson junctions", Phys. Rev. Lett. 67: 255 (1991).

[UE1b] R.Graham, M.Schlautmann, P.Zoller, "Dynamical localization of atomic-beam deflection by a mudulated standing light wave", Phys. Rev. A 45: R19 (1992).

[UE1c] F.L.Moore, J.C.Robinson, C.Bharucha, P.E.Williams, M.G.Raizen, "Observation of dynamical localization in atomic momentum transfer: a new testing ground for quantum chaos", Phys. Rev. Lett. 73: 2974 (1994).

[UE2a] C.Ryu, M.F.Anderson, A.Vaziri, M.B.d'Arcy, J.M.Grossman, K.Helmerson, W.D.Phillips, "High-order quantum resonances observed in a periodically kicked Bose-Einstein condensate", Phys. Rev. Lett. 96: 160403 (2006).

[UE2b] J.Kanem, S.Maneshi, M.Partlow, M.Spanner, A.M.Steinberg, "Observation of high-order quantum resonances in the kicked rotor", Phys. Rev. Lett. 98: 083004 (2007).

[UE3a] L. Boltzmann. "Über die Beziehung eines allgemeine mechanischen Satzes zum zweiten Haupsatze der Wärmetheorie". *Sitzungsberichte der Akademie der Wissenschaften*, Wien, Vol. II 75, pp. 67-73 (1877).

[UE3b] J. Loschmidt. "Über den Zustand des Wärmegleichgewichts eines Systems von Körpern mit Rücksicht auf die Schwerkraft", *Sitzungsberichte der Akademie der Wissenschaften*, Wien, Vol. II 73, pp. 128-142 (1876).

[UE3c] J.Martin, B.Georgeot, D.L.Shepelyansky, "Time reversal of Bose-Einstein condensates", Phys. Rev. Lett. 101: 074102 (2008).

[UE3d] A.Ullah, M.D.Hoogerland, "Experimental observation of Loschmidt time reversal of a quantum chaotic system", Phys. Rev. E 83: 046218 (2012).

[UE4a] D.L.Shepelyansky, "Anderson transition in three and four effective dimensions for the frequency modulated kicked rotator", arXiv:1102.4450(cond-mat.dis-nn) (2011).

[UE4b] J.-C.Garreau, "Quantum simulation of disordered systems with cold atoms", Comptes Rendus Physique 18: 31 (2017).

[UE4c] J.P.Dahlhaus, J.M.Edge, J.Tworzydlo, C.W.J.Beenakker, "Quantum Hall effect in a one-dimensional dynamical system", Phys. Rev. B 84: 115133 (2011).

[UE4d] J.M.Edge, J.Tworzydlo, C.W.J.Beenakker, "Metallic phase of the quantum Hall effect in four-dimensional space", Phys. Rev. Lett. 109: 135701 (2012).

[UE4e] C.Tian, Y.Chen, J.Wang, "Emergence of integer quantum Hall effect from chaos", Phys. Rev. B 93: 075403 (2016).

[UE4f] H.S.Yamada, F.Matsui, K.S.Ikeda, "Critical phenomena of dynamical delocalization in a quantum Anderson map", Phys. Rev. E 92: 062908 (2015).

[UE5a] J.Flob, A.Kamalov, I.S.Averbukh, P.H.Bucksbaum, "Observation of Bloch oscillations in molecular rotation", Phys. Rev. Lett. 115: 203002 (2015).

[UE5b] M.Bitter, V.Milner, "Experimental observation of dynamical localization in laser-kicked molecular rotors", Phys. Rev. Lett. 117: 144104 (2016).

[UE5c] M.Bitter, V.Milner, "Experimental demonstration of coherent control in quantum chaotic systems", Phys. Rev. Lett. 118: 034101 (2017).

[UE6a] A.Bylinskii, D.Gangloff, I.Countis, V.Vuletic, "Observation of Aubry-type transition in finite atom chains via friction", Nat. Mater. 11: 717 (2016).

[UE6b] J.Kiethe, R.Nigmatullin, D.Kalincev, T.Schmirander, T.E.Mehlstaubler, "Probing nanofriction and Aubry-type signatures in a finite self-organized system", Nat. Comm. 8: 15364 (2017).

[UE6c] N.Manini, G.Mistura, G.Paolicelli, E.Tosatti, A.Vanossi, "Current trends in the physics of nanoscale friction" Adv. Phys. X 2(3): 569 (2017).

[UE6d] O.V.Zhirov, D.L.Shepelyansky, "Thermoelectricity of Wigner crystal in a periodic potential", EPL 103: 68008 (2013).

[UE6e] O.V.Zhirov, J.Lages, D.L.Shepelyansky, "hermoelectricity of cold ions in optical lattices", Eur. Phys. J. D 73: 149 (2019).

[UE6f] A.F.Ioffe, "Semiconductor thermoelements and thermoelectric cooling", Infosearch, London (1957).

[UE6g] S.Bang, D.Wee, A.Li, A.Fornari, B.Kozinsky, "Thermoelectric properties of pnictogen-substituted skutterudites with alkaline-earth fillers using first-principles calculations", Jour. Appl. Phys. 119: 205102 (2016).

[UE7a] A.D.Chepelianskii, D.L.Shepelyansky, "Microwave stabilization of edge transport and zero-resistance states", Phys. Rev. B 80: 241308(R) (2009).

[UE7b] A.D.Levin, Z.S.Momtaz, G.M.Gusev, A.K.Bakarov, "Microwave-induced nonlocal transport in a two-dimensional electron gas", Phys. Rev. B 89: 161304(R) (2014).

[UF1a] N.Bohr, "Uber die Serienspektra der Element", Zeitschrift fur Physik 2(5): 423 (1920); https://doi.org/10.1007/BF01329978

[UF1b] P.Ehrenfest, "Bemerkung uber die angenaherte Gultigkeit der klassischen Mechanik innerhalb der Quantenmechanik", Zeitschrift fur Physik 45(7-8): 455 (1927); https://doi.org/10.1007/BF01329203

[UF1c] D.L.Shepelyanskii, "Quasiclassical approximation for stochastic quantum systems", Soviet Physics Doklady 26: 80 (1981); Preprint INP 80-132, Dated April 7, 1980, Novosibirsk.

[UF1d] G.P.Berman, G.M.Zaslavsky, "Condition of stochasticity in quantum nonlinear systems", Physica A 91: 450 (1978).

[UF4a] J.D.Meiss, E.Ott, "Markov-tree model of intrinsic transport in Hamiltonian systems", Phys. Rev. Lett. 55: 2741 (1985).

[UF6a] B.V.Chirikov, D.L.Shepelyanskii, "Dynamics of some homogeneous models of classical Yang-Mills fields", Sov. J. Nucl. Phys. 36(6): 908 (1982); [28] (http://www.quantware.ups-tlse.fr/dima/myrefs/my008.pdf) .

[UF7a] A.S.Pikovsky, D.L.Shepelyansky, "Destruction of Anderson localization by a weak nonlinearity", Phys. Rev. Lett. 100: 094101 (2008).

[UF7b] M.Mulansky, A.Pikovsky, "Energy spreading in strongly nonlinear disordered lattices", New J. Phys. 15: 053015 (2013).

[UF7c] T.V.Lapteva, M.I.Ivanchenko, S.Flach, "Nonlinear lattice waves in heterogeneous media", J. Phys. A: Math. Theor. 47: 493001 (2014).

[UF7d] I.Vakulchyk, M.V.Fistul, S.Flach, "Wave packet spreading with disordered nonlinear discrete-time quantum walks", Phys. Rev. Lett. 122: 040501 (2019).

[UF7e] I.Garcia-Mata, D.L.Shepelyansky, "Delocalization induced by nonlinearity in systems with disorder", Phys. Rev. E 79: 026205 (2009).

See also added after 2008

Anderson localization and quantum chaos maps, Chirikov criterion, Cold atom experiments in quantum chaos, Google matrix, Kicked cold atoms in gravity field, kicked Harper model, Microwave ionization of hydrogen atoms, Kepler map

Sponsored by: Eugene M. Izhikevich, Editor-in-Chief of Scholarpedia, the peer-reviewed open-access encyclopedia

Sponsored by: Prof. James Meiss, Applied Mathematics University of Colorado, Boulder, CO, USA

Reviewed by (http://www.scholarpedia.org/w/index.php?title=Chirikov_standard_map&oldid=32317) : Prof. Allan Lichtenberg, Electrical Engineering, Univ. of California at Berkeley

Reviewed by (http://www.scholarpedia.org/w/index.php?title=Chirikov_standard_map&oldid=32317) : Anonymous

Accepted on: 2008-03-03 19:08:51 GMT (http://www.scholarpedia.org/w/index.php?title=Chirikov_standard_map&oldid=34128)

Categories: Mappings | Eponymous | Quantum Chaos | Multiple Curators